Three-Dimensional Position Control using Sliding Mode Control for Multi-Input Systems

João Filipe Silva
MP-273: Sliding Mode Control

June 6, 2021

Abstract

This document contains the second computational exercise for the Sliding Mode Control (SMC) class. Based on the content given in the lectures, it was requested to formulate an algorithm capable of representing a underactuated Multirotor Aerial Vehicle (MAV) whose three-Dimensional Position and Velocity were to be controled by an Adaptive SMC method. The controller was implemented in Matlab scripts[1] and plots were generated to illustrate the errors between the real states and their commanded values.

1 Problem Formulation

Consider an underactuated multicopter, represented in practice by drones or eVTOL aircrafts with fixed rotors (non-vectorable and with constant pitch). These vehicles have cascaded translation and rotation dynamics, in such a way that the translation is affected by the rotation, but not the other way around. Their underactuation characteristic refers to the fact that, albeit having movement in six degrees of freedom (three-dimensional position and attitude), only four independent control efforts (magnitude of the resulting thrust and torque on three axes) are applied. As reported in the literature [1], a simple way to deal with this dynamic characteristic is through a hierarchical control structure, in which the attitude control loop is placed internally to the position control loop. Thus, as long as it is possible in practice to make the rotation dynamics much faster than the translation dynamics, both in a closed loop, it is possible to satisfactorily design the laws of translation and rotation control separately.

In this work, only the translational control law design will be addressed. Initially, consider two Cartesian Coordinate Systems (CCS), as shown in Figure 1. The body CCS $\mathcal{S}_b \triangleq \{B; \vec{x}_b; \vec{y}_b; \vec{z}_b\}$ is attached to the MAV (supposedly rigid) structure, with its origin at the MAV center of mass denoted by B, the $\vec{x}_b$ axis pointing forwards, the $\vec{z}_b$ axis normal to the vehicle's structure and pointing upwards, and the $\vec{y}_b$ axis completing an orthonormal dextrogirous basis of the three-dimensional space. The ground (or global) CSS $\mathcal{S}_g \triangleq \{G; \vec{x}_g; \vec{y}_g; \vec{z}_g\}$ is attached to a known point G on the ground, with the $\vec{z}_b$ axis normal to the surface and pointing upwards, and the remaining axes arbitrarily oriented, while satisfying the assumption that they also constitute orthonormal dextrogirous basis of the three-dimensional space. Figure 1 also illustrates the MAV position vector $\vec{r}^{b/g}$, here represented as the position of $\mathcal{S}_b$ with respect to $\mathcal{S}_g$.

[1] All scripts can be found in: https://github.com/jfilipe33/ExCompMP273

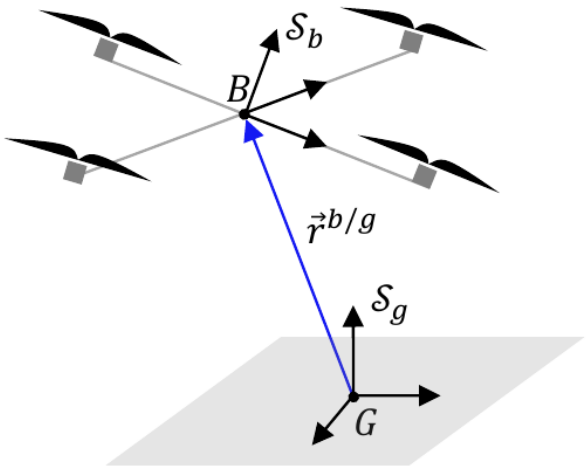

Figure 1: Graphic representation of a underactuated MAV.

Consider that the vehicle has constant mass m and suppose that $\mathcal{S}_g$ represents an itertial reference. Therefore, Newton's Second Law of Motion describes the body movement as:

$$m\frac{^g d^2}{dt}\vec{r}^{b/g} = \vec{f}^{g} + \vec{f}^{c} + \vec{f}^{d}, \tag{1}$$

where $\vec{f}^{g}$, $\vec{f}^{c}$, and $\vec{f}^{d}$ denote the gravity, control and disturbance force vectors, respectively. The superindex g, to the left of the time derivative, indicates that this one is taken with respect to a observer on $\mathcal{S}_g$.

In the translational controller design, instead of using equation (1), which is expressed in Euclidian vectors, it is more convenient to represent the motion in algebric form. Therefore, once each geometric vector in (1) is represented in $\mathcal{S}_g$, we have:

$$m\ddot{\mathbf{r}}_g^{b/g} = \mathbf{f}_g^{g} + \mathbf{f}_g^{c} + \mathbf{f}_g^{d} \tag{2}$$

Finally, assuming $\mathbf{f}_g^{g} \triangleq -mg\mathbf{e}_3$, where g denotes the gravity acceleration magnitude, and $\mathbf{e}_3 \triangleq (0,0,1)$, we obtain:

$$\ddot{\mathbf{r}}_g^{b/g} = -g\mathbf{e}_3 + \frac{1}{m}\mathbf{f}_g^{c} + \frac{1}{m}\mathbf{f}_g^{d} \tag{3}$$

The objective of this exercise is to formulate a Sliding Mode Controller that makes the MAV, whose dynamics are described in (3), follow a desired trajectory even when perturbed by a unknown, but bounded, disturbance signal.

2 Problem Analysis

Let us start by representing the system dynamics, described in equation (3), in State Space regular form for non-linear systems.

$$\begin{aligned} \dot{\mathbf{x}}_1 &= \mathbf{f}_1(\mathbf{x}_1, \mathbf{x}_2) \\ \dot{\mathbf{x}}_2 &= \mathbf{f}_2(\mathbf{x}_1, \mathbf{x}_2) + \mathbf{B}(\mathbf{x}_1, \mathbf{x}_2)(\mathbf{u} + \mathbf{d}) \end{aligned} \tag{4}$$

where $\mathbf{x}_1 \triangleq \mathbf{r}_g^{b/g}$, $\mathbf{x}_2 \triangleq \dot{\mathbf{r}}_g^{b/g}$, $\mathbf{u} \triangleq \mathbf{f}_g^{c}$, and $\mathbf{d} \triangleq \mathbf{f}_g^{d}$.

From (3) and (4), we obtain $\mathbf{B} = \frac{1}{m}$ and:

$$\begin{aligned} \mathbf{f}_1(\mathbf{x}) &= \mathbf{x}_2 \\ \mathbf{f}_2(\mathbf{x}) &= -g\mathbf{e}_3 \end{aligned} \tag{5}$$

The tracking error dynamics can also be modelled in State Space regular form. For that, let us assume $\tilde{\mathbf{x}}_1 \triangleq \mathbf{x}_1 - \bar{\mathbf{r}}_g^{b/g}$ and $\tilde{\mathbf{x}}_2 \triangleq \mathbf{x}_2 - \dot{\bar{\mathbf{r}}}_g^{b/g}$, where $\bar{\mathbf{r}}_g^{b/g}$ represents the desired trajectory. From (3), (4) and the definitions above:

$$\begin{aligned} \dot{\tilde{\mathbf{x}}}_1 &= \tilde{\mathbf{x}}_2 \\ \dot{\tilde{\mathbf{x}}}_2 &= -g\mathbf{e}_3 - \ddot{\bar{\mathbf{r}}}_g^{b/g} + \tfrac{1}{m}(\mathbf{u} + \mathbf{d}) \\ \mathbf{f}_1(\tilde{\mathbf{x}}) &= \tilde{\mathbf{x}}_2 \\ \mathbf{f}_2(\tilde{\mathbf{x}}) &= -g\mathbf{e}_3 - \ddot{\bar{\mathbf{r}}}_g^{b/g} \end{aligned} \tag{6}$$

Let us consider the following assumptions:

- $\frac{\partial \mathbf{f}_1}{\partial \mathbf{x}_2}(\mathbf{x})\mathbf{B}(\mathbf{x}) \neq 0, \quad \forall \mathbf{x}$
- $\left\| \frac{\partial \mathbf{f}_1}{\partial \mathbf{x}_2}(\mathbf{x})\mathbf{B}(\mathbf{x}) \right\| \geq \mu > 0, \quad \forall \mathbf{x}$
- $\|\mathbf{d}\| \leq \rho$, with unknown $\rho > 0$.

The control objective is to design an adaptive control law $\mathbf{u} = \nu(\tilde{\mathbf{x}})$ that makes $\tilde{\mathbf{x}} = 0$ a global asymptotically stable equilibrium point of (6), without previous knowledge of the disturbance upper bound, while the switching gain converges to a constant maximum value κ_{max}. For such a task, lets define the sliding variable as:

$$\sigma(\tilde{\mathbf{x}}) \triangleq \mathbf{C}\tilde{\mathbf{x}}_1 + \mathbf{f}_1(\tilde{\mathbf{x}}) \in \mathbb{R}^3 \tag{7}$$

where $\mathbf{C} \in \mathbb{R}^{3\times 3}$ is a given diagonal positive definite (PD) matrix. Lets also define the corresponding elementary sliding surfaces:

$$\mathcal{S}_i \triangleq \{\tilde{\mathbf{x}} \in \mathbb{R}^n : \sigma_i(\tilde{\mathbf{x}}) = 0\}, \quad i = 1, 2, 3$$

where $s_i(\mathbf{x})$ denotes the ith component of $\mathbf{s}(\mathbf{x})$.

In particular, the intersection of all the elementary sliding surfaces is called the eventual sliding surface and is denoted by:

$$\mathcal{S} \triangleq \mathcal{S}_1 \cap \mathcal{S}_2 \cap \mathcal{S}_3$$

The sliding motion on $\mathcal{S}$ is called eventual sliding mode; its dynamics are such that $\sigma(\tilde{\mathbf{x}}) = \mathbf{0}$, which from (7) implies

$$\dot{\tilde{\mathbf{x}}}_1 = -\mathbf{C}\tilde{\mathbf{x}}_1 \tag{8}$$

As C is a diagonal and PD by definition, by solving the differential equation in (8), it's possible to see that $(\tilde{\mathbf{x}}_1, \dot{\tilde{\mathbf{x}}}_1) \to \mathbf{0}$ exponentially. As $\tilde{\mathbf{x}}_1 \to \mathbf{0}$, then, from (6), $\mathbf{f}_1(\tilde{\mathbf{x}}) \to \mathbf{0}$ exponentially. Consequently, $\tilde{\mathbf{x}}_2 \to \mathbf{0}$ exponentially. Therefore, it's possible to assert that $(\tilde{\mathbf{x}}_1, \tilde{\mathbf{x}}_2) \to \mathbf{0}$ exponentially and $\tilde{\mathbf{x}} = \mathbf{0}$ is an exponentially stable equilibrium point of (6).

For this exercise, the Eventual switching scheme was chosen, in which control law is designed to make $\tilde{\mathbf{x}}$ directly reach the eventual sliding surface $\mathcal{S}$, *i.e.*, it makes $\|\sigma\| \to \mathbf{0}$ in finite time.

The dynamics of σ are obtained by differentiating (7) with respect to time, resulting in:

$$\begin{aligned} \dot{\sigma}(\tilde{\mathbf{x}}) &\triangleq \mathbf{C}\mathbf{f}_1(\tilde{\mathbf{x}}) + \mathbf{f}_2(\tilde{\mathbf{x}}) + \mathbf{B}(\mathbf{u} + \mathbf{d}) \\ \dot{\sigma}(\tilde{\mathbf{x}}) &\triangleq \mathbf{C}\tilde{\mathbf{x}}_2 - g\mathbf{e}_3 - \ddot{\bar{\mathbf{r}}}_g^{b/g} + \tfrac{1}{m}(\mathbf{u} + \mathbf{d}) \end{aligned} \tag{9}$$

For this exercise, lets assume the following given vectors:

$$\mathbf{d}(t) = \begin{bmatrix} 0,3\sin(\pi t/4) \\ 0,4\sin(\pi t/4+\pi/2) \\ 0,5\sin(\pi t/4+\pi) \end{bmatrix} N \qquad \bar{\mathbf{r}}_g^{b/g}(t) = \begin{bmatrix} \sin(\pi t/2) \\ \sin(\pi t/2+\pi/2) \\ t/4 \end{bmatrix} \text{m}$$

When plotting the Phase Portrait of the disturbance vector, figure 2 is obtained. From it, it's possible to see that magnitude of the disturbance vector reaches its maximum value at the points $[-0.3, 0, 0.5]$ and $[0.3, 0, -0.5]$. Said magnitude is obtained by taking the 2-norm of the vector at said points, and it's denoted by $\rho = \|[-0.3;\ 0;\ 0.5]\|_2 = 0.5831$. However, the control law has to be able to make $\tilde{\mathbf{x}} = 0$ a global asymptotically stable equilibrium point of (6) without previous knowledge of ρ.

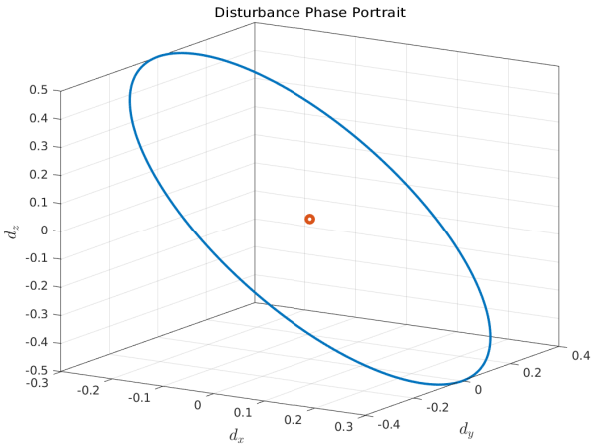

Figure 2: Disturbance Phase Portrait

The control law

$$\begin{aligned} \mathbf{u} &= -m\left(\mathbf{C}\tilde{\mathbf{x}}_2 - g\mathbf{e}_3 - \ddot{\bar{r}}_g^{b/g} + \frac{1}{m}\kappa(t)\frac{\sigma}{\|\sigma\|}\right) \\ \dot{\kappa} &= \gamma\|\sigma\|\mathbb{I}_{\mathcal{E}}(\|\sigma\|) \end{aligned} \tag{10}$$

with $\kappa(0) \geq 0$ and $\mathcal{E} \triangleq \mathbb{R}\backslash[-\varepsilon, \varepsilon]$, ensures that:

- $\sigma = \mathbf{0}$ is a global finite-time-stable (GFTS) equilibrium point of the σ dynamics
- $\kappa(t) \to \kappa_{max} < \infty$ in finite time

To prove that the control law $\mathbf{u}$ in (10) makes $(\sigma(\tilde{\mathbf{x}}), \tilde{\kappa}) = (\mathbf{0}, 0)$, where $\tilde{\kappa} = \kappa(t) - \kappa_{max}$, a GFTS equilibrium point of (9), lets consider the following Lyapunov candidate function:

$$V_\sigma(\sigma) = \frac{1}{2}\left(\|\sigma\| + |\tilde{\kappa}|\right)^2 \tag{11}$$

Now, lets calculate the time derivative of (11):

$$\begin{aligned} \dot{V}_\sigma(\sigma) &= \frac{1}{2} \times 2 \times \left(\|\sigma\| + |\tilde{\kappa}|\right) \times \frac{d}{dt}\left(\|\sigma\| + |\tilde{\kappa}|\right) \\ &= \left(\|\sigma\| + |\tilde{\kappa}|\right)\left(\frac{\sigma^T\dot{\sigma}}{\|\sigma\|} + \dot{\tilde{\kappa}}sign(\tilde{\kappa})\right) \end{aligned} \tag{12}$$

From (11) it is possible to see that $\left(\|\sigma\| + |\tilde{\kappa}|\right) = \sqrt{2}V_\sigma(\sigma)^{1/2}$. Also, since κ_{max} is a constant value, $\dot{\tilde{\kappa}} = \dot{\kappa}$. In addition, $sign(\tilde{\kappa}) \leq 0$, as $\kappa_{max} \geq \kappa$. Therefore, by substituting (9) and (10) and with some mathematical manipulation, the equation (12) can be rewritten as:

$$
\begin{aligned}
\dot{V}_\sigma(\sigma) &= \sqrt{2}V_\sigma(\sigma)^{1/2}\left(\frac{\sigma^T}{\|\sigma\|}\left(\mathbf{C}\tilde{\mathbf{x}}_2 - g\mathbf{e}_3 - \ddot{\mathbf{r}}_g^{b/g} + \frac{1}{m}(\mathbf{u}+\mathbf{d})\right) + \gamma\|\sigma\|\mathbb{I}_{\mathcal{E}}(\|\sigma\|)sign(\tilde{\kappa})\right) \\
&= \sqrt{2}V_\sigma(\sigma)^{1/2}\left(\frac{\sigma^T}{\|\sigma\|}\left(-\frac{1}{m}\kappa(t)\frac{\sigma}{\|\sigma\|} + \frac{1}{m}\mathbf{d}\right) + \gamma\|\sigma\|\mathbb{I}_{\mathcal{E}}(\|\sigma\|)sign(\tilde{\kappa})\right) \\
&\leq -\frac{1}{m}\sqrt{2}V_\sigma(\sigma)^{1/2}\left(\kappa(t) - \frac{\|\sigma^T\|}{\|\sigma\|}\|\mathbf{d}\|\right) \\
\dot{V}_\sigma(\sigma) &\leq -\frac{1}{m}\sqrt{2}V_\sigma(\sigma)^{1/2}\left(\kappa(t) - \rho\right)
\end{aligned}
\tag{13}
$$

From the Bhat-Bernstein Theorem, for $\alpha \in (0,1)$, V radially unbounded e $\dot{V}$ globally negative definite, if there is $\eta > 0$ such that

$$
\dot{V}(x) + \eta V(x)^{1-\alpha} \leq 0, \quad \forall x \in \mathbb{R}^{n_x} \tag{14}
$$

then $x = 0$ is globally finite-time stable.

By rearranging equation (13), we obtain:

$$
\begin{aligned}
&\dot{V}_\sigma(\sigma) + \frac{1}{m}\sqrt{2}V_\sigma(\sigma)^{1/2}\left(\kappa(t) - \rho\right) \leq 0 \\
&\therefore \eta = \frac{\sqrt{2}}{m}\left(\kappa(t) \ - \rho\right) \quad and \quad \alpha = 1/2
\end{aligned}
\tag{15}
$$

If there is exists an instant $t^* < \infty$ such as η is positive (*i.e.* $\kappa(t) > \rho$) $\forall t \geq t^*$, $(\sigma(\tilde{\mathbf{x}}), \tilde{\kappa}) = (\mathbf{0}, 0)$ will be a GFTS equilibrium point of (9). Let us verify that $\|\sigma\|$ increases as long as $\kappa(t) < \frac{\sigma^T}{\|\sigma\|}\mathbf{d}$:

$$
\begin{aligned}
\frac{d}{dt}\|\sigma\| &= \frac{\sigma^T}{\|\sigma\|}\left(-\frac{1}{m}\kappa(t)\frac{\sigma}{\|\sigma\|} + \frac{1}{m}\mathbf{d}\right) \\
&= \frac{1}{m}\left(\frac{\sigma^T}{\|\sigma\|}\mathbf{d} - \kappa(t)\right)
\end{aligned}
\tag{16}
$$

From (16), if $\kappa(t) < \frac{\sigma^T}{\|\sigma\|}\mathbf{d}$, there will exist a finite instant $t_{\mathcal{E}}$ such that $\|\sigma(t_{\mathcal{E}})\| > \varepsilon$. According to the adaptation law in (10), for $t > t_{\mathcal{E}}$, the switching gain $\kappa(t)$ increases monotonically until $\|\sigma(t_{\mathcal{E}})\| \leq \varepsilon$ again. This instant will be denoted as t_s. But to achieve t_s, there has to exist an instant $t^* = t_{\mathcal{E}} + \Delta t < t_s$ in which $\kappa(t^*) > \frac{\sigma^T}{\|\sigma\|}\mathbf{d}$, and $\|\sigma\|$ starts to decrease. As $\mathbf{d}$ is bounded, it is possible to say that $\Delta t < \infty$ exists and, therefore, $t^* < \infty$ also exists.

Now let us consider that sliding mode is reached at instant $t_s < \infty$. The switching gain can be calculated using the adaptation law in (10), in the following form:

$$
\kappa(t) = \kappa(t_s) + \gamma\int_{t_s}^{t}\|\sigma(\tau)\|\mathbb{I}_{\mathcal{E}}(\|\sigma(\tau)\|)d\tau \tag{17}
$$

If the boundary ε is correctly chosen, the chattering effect of $\|\sigma(t)\|$ shall remain inside $[-\varepsilon, \varepsilon]$. Therefore, from (17):

$$
\begin{aligned}
\kappa(t) &= \kappa(t_s) + \gamma\int_{t_s}^{t}\|\sigma(\tau)\| \times 0 \ d\tau \\
\therefore \kappa(t) &= \kappa(t_s), \quad \forall t \geq t_s
\end{aligned}
\tag{18}
$$

Since at t_s the switching gain reaches its maximum value, $\tilde{\kappa}(t) = \kappa(t_s) - \kappa_{max} = 0, \ \forall t \geq t_s$.

3 System Simulation

The MAV used in this simulation will have $m = 1kg$, and we'll consider $g = 9.81m/s^2$ and $\mathbf{C} = \mathbf{I}_3$. For a initial switching gain of $\kappa(0) = 0$, $\gamma = 1$, $\varepsilon = 0.005$ and $Ts = 0.0001s$, these are the plots obtained:

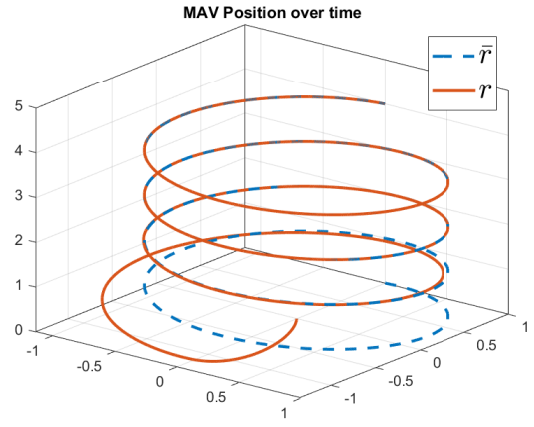

(a) MAV Position over time

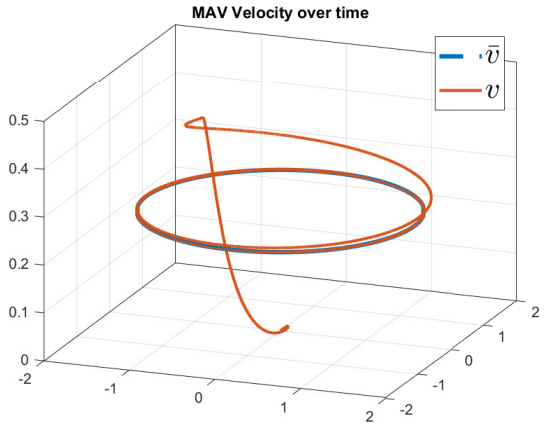

(b) MAV Velocity over time

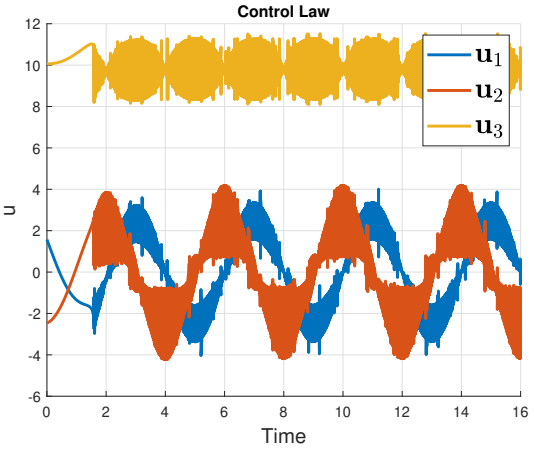

(c) Control Law u

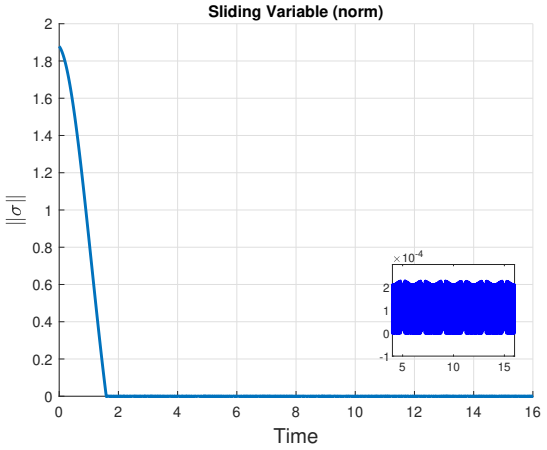

(d) Sliding Variable $\|\sigma\|$

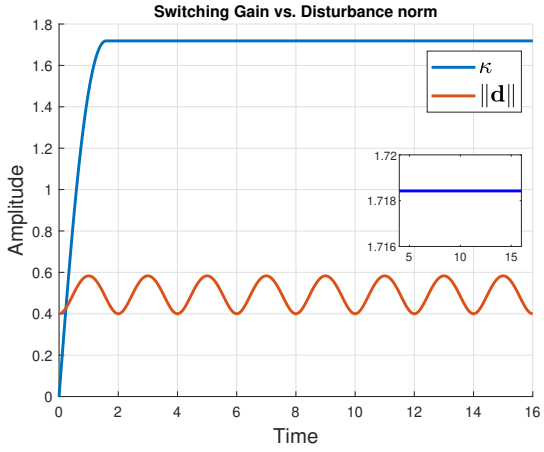

(e) Switching Gain $\kappa(t)$

Figure 3: MAV Position tracking using ASMC.

In figure 3d it is possible to see that the system reaches sliding mode at $t_s \approx 1.6s$. The 3D position and velocity are tracked with considerable accuracy as seen in figures 3a and 3b, while the control law $\mathbf{u}$ switches with high frequency when sliding mode is reached, as seen in figure 3c. As mentioned before, this exercise employs the eventual sliding mode, which means every component of σ, and consequently $\|\sigma\|$, reaches sliding mode simultaneously, which is also illustrated in figure 3d. Figure 3e shows that the switching gain increases until the system reaches sliding mode. For the chosen parameters and initial values, the gain has settled at $\kappa(t_s) \approx 1.718$. From equation (15), we know that $\kappa(t)$ only needs to be greater than ρ for the system to reach finite-time stability. But the adaptation law makes κ increase much more than necessary and, although we achieve stability, it is at the cost of an over-dimensioned switching gain. For the next simulation, the value of γ will be reduced tenfold to evaluate how a slower gain adaptation will affect the MAV behaviour.

In figure 4d it is possible to see that the system reaches sliding mode at $t_s \approx 5.8s$. The 3D position and velocity take a longer amount of time to be tracked with considerable accuracy as seen in figures 4a and 4b, while the control law $\mathbf{u}$ switches with high frequency when sliding mode is reached, as seen in figure 4c. Figure 4e shows that the switching gain increases until the system reaches sliding mode. For the chosen parameters and initial values, the gain has settled at $\kappa(t_s) \approx 0.6$. As the plots show, the cost of the low value of $\kappa(t_s)$ was a much longer reaching phase and poor initial behavior of the MAV position while trying to track the commanded values.

As commented before in this report, the value of ε has to be high enough to surround the chattering effect on the sliding variable σ during sliding mode. As seen in figures 3d and 4d, $\|\sigma\| < 2 \times 10^{-4}$, $\forall t > t_s$. Therefore, the region $[-\varepsilon, \varepsilon]$, for $\varepsilon = 0.005$, is large enough so that $\|\sigma\|$ does not leave it because of the chattering effect. In case this condition was not satisfied, from the second equation in (10), it is clear that $\dot{\kappa}$ would be positive and, consequently, κ would continue to increase, even though sliding mode was reached.

In conclusion, the ASMC algorithim designed was able to take the position error to zero in finite-time without previous knowledge of the disturbance upper bound, which was needed for the conventional SMC algorithim. However, this comes at the cost of an over-dimensioned switching gain. Some of the options to reduce κ_{max} is to reduce the parameter γ, making the adaptation law slower; moving the initial position $\mathbf{r}_g^{b/g}(0)$ closer to the initial commanded position $\bar{\mathbf{r}}_g^{b/g}(0)$; or reducing the mass of the MAV.

References

[1] Silva, A. L.; Santos, D. A. Fast Nonsingular Terminal Sliding Mode Flight Control for Multirotor Aerial Vehicles. IEEE Transactions on Aerospace and Electronic Systems, 56(6), 2020.

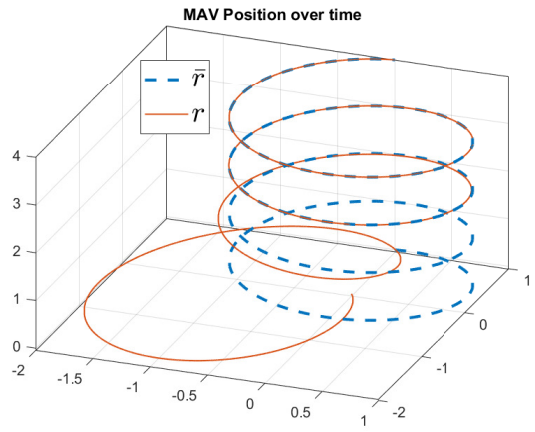

(a) MAV Position over time

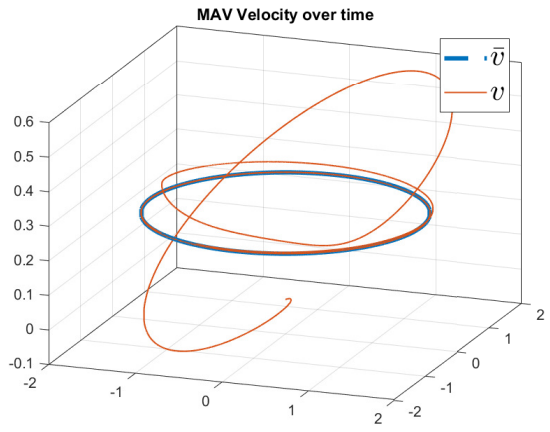

(b) MAV Velocity over time

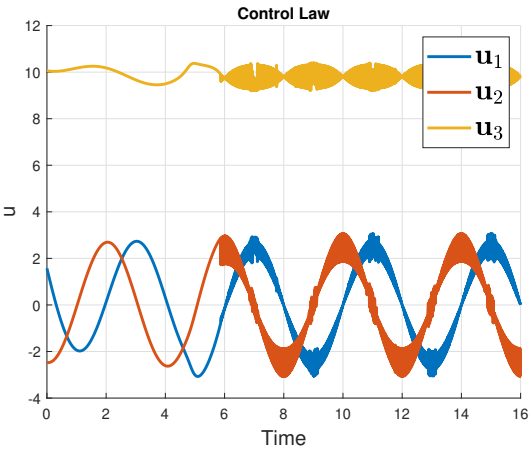

(c) Control Law u

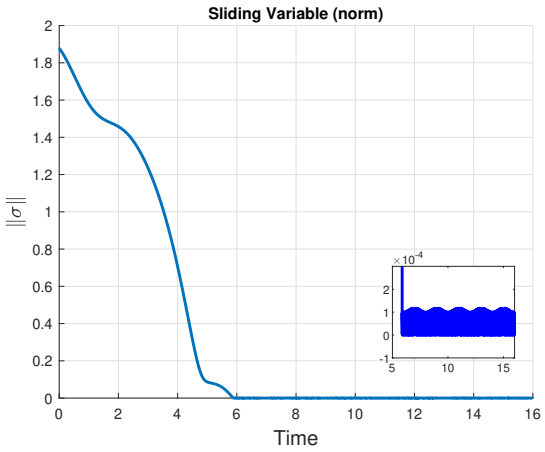

(d) Sliding Variable $\|\sigma\|$

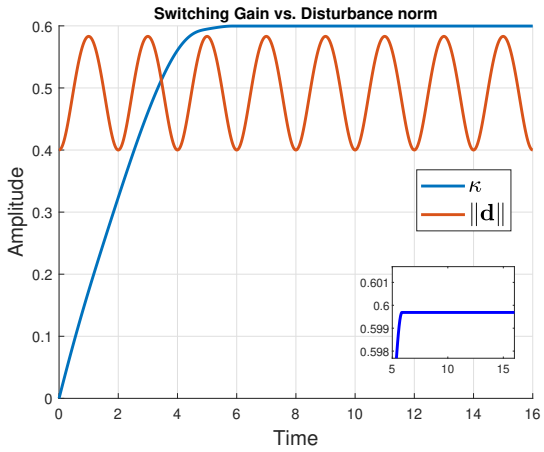

(e) Switching Gain $\kappa(t)$

Figure 4: MAV Position tracking using ASMC.